CEIG - Spanish Computer Graphics Conference (2018)
I. García-Fernández and C. Ureña (Editors)

A Physically-Based Spatio-Temporal Sky Model

David Guimera Diego Gutierrez Adrian Jarabo

Universidad de Zaragoza, I3A

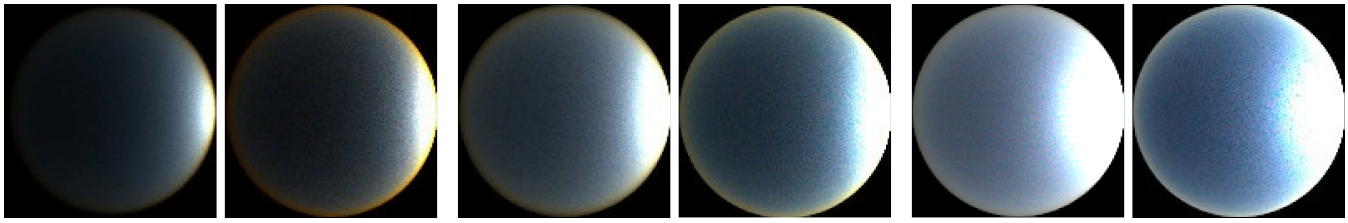

Figure 1: Effect of the location of the observer on the apperance of the atmosphere for different sun elevations. From left to right, URBAN and RURAL atmospheres with sun elevation at 0°, DESERT and CLEAN MARITIME with sun elevation at 5°, and URBAN and POLAR ARTIC with sun elevation at 25°. All renders are set to January, and with the same atmosphere turbidity.

Abstract

In this work we present a physically-based optical model of the atmosphere, that takes into account the seasonal and geographic variation of its composition. Based on data from the atmospheric science literature, we build a highly detailed the composition of the atmosphere, and how it varies depending on the position of the observer, or the time of the year. Then, based on precise measurements of the optical properties of the components of the atmosphere, we map our model into a radiative model, which can be rendered in any existing volumetric renderer. We demonstrate our model in multispectral renders of daylight sky-domes, showing the changes in the appearance occurring when varying the season or location of the observer.

1. Introduction

Rendering the appearance of the atmosphere is a long-standing problem in computer graphics, given its importance in a number of applications, from architecture and ergonomics, to movies or videogames. The color of the sky is the consequence of the complex interactions between light and the gases and suspended particles that form the atmosphere. Thus, for accurately depicting the sky we need to precisely model both the contributing light sources (mainly the Sun, but also zodiacal light, starlight, or the light reflected by the Moon or space dust [JDD*01]), and the composition of the atmosphere.

Several works have tackled the problem of modeling the appearance of the sky, either by proposing parametric analytical models [PSS99, HW12], or by accurately modeling the structure of the atmosphere and performing costly light transport simulations [NDKY96, HMS05]. However, most of these works assume an idealized average atmosphere, which presents the same composition, and therefore appearance, regardless of the particular season or the position of the observer. This uniformity is a strong assumption, given the seasonal changes on the atmosphere composition, and the human and environmental effects on the lower parts of the atmosphere, specially on the composition of aerosols.

In this work, we present the first steps for incorporating such spatio-temporal variability on the appearance of the sky, by developing a fine-grained atmospheric model based on detailed description of the composition of the atmosphere. Our model bases on a thorough review of the atmospheric science literature, from which we gather precise measurements of the distribution of the atmosphere molecules (e.g. nitrogen, oxygen, or ozone) and suspended aerosols, as a function of location and time of the year. We then transform our description of the atmosphere into optical parameters, which can be directly plugged into the radiative transfer theory [Cha60], and rendered with any volumetric rendering method [NGHJ18].

Our main contribution is an accurate model of the composition of the atmosphere as a function of the time of the year and the particular location of the observer. We build our model on a measurements from atmospheric science, finding the parameters in the atmosphere that are more sensitive to the spatial location and seasonal changes, and modeling such variation. Then we map these to an optical description of the atmosphere usable for rendering. We

demonstrate spectral daylight renderings of the atmosphere under a variety of geographic locations (including e.g. polar, urban, or dessert conditions) and times of the year, and analyze how taking into account the different composition of the atmosphere affects the appearance of the sky.

2. Related Work

Light transport in the atmosphere is a well studied problem in several fields, including atmospheric science or remote sensing. Here we focus only on works within computer graphics, and refer to other sources for details in other domains [TS99]. Additionally, for an in-depth, empirical comparison of the most relevant models described here, we refer to the works of Kider et al. [KJKN*14] and Bruneton [Bru17].

Explicit models The most versatile approach for rendering the atmosphere is to model with fine detail the distribution of the suspended scattering particles, and explicitly simulating how light interacts with them; for details on volumetric rendering we refer to a recent survey on the topic [NGHJ18]. The first model following this approach was proposed by Nishita et al. [NSTN93], which accounted for molecules and aerosols in the atmosphere, but was restricted to single scattering. Later, this model was extended to incorporate multiple scattering, by tabulating the distribution of radiance in the atmosphere to accelerate computations [NDKY96]. These works rely on brute-force light transport simulations, and are very slow. To accelerate rendering, Bruneton and Neyret [BN08] and Elek and Knoch [EK10] proposed to precompute the radiance distribution on the atmosphere, making their models suitable for the GPU. Based on Nishita's model of the atmosphere, O'Neil [O'N05] developed an accurate real-time method for simulating the sky, limited to single scattering. Nishita's atmospheric model was also used by Jensen and colleagues [JDD*01] to develop an accurate night sky model which includes light from the Moon, bright stars or celestial light. Based on measured data, Haber et al. [HMS05] proposed an accurate model for the atmosphere, able to precisely simulate the complex color distributions on the sky during twilight. Their model accounts not only for distribution of scatterers, but also for humidity and temperature, which results in bent light rays due to continuously-varying index of refraction, which has an important effect in twilight conditions. Gutierrez et al. [GSAM04] also accounted the the curvature of light rays, showing effects such as mirages, Fata Morganas, or the Green Flash. Kutz [Kut12] proposed an accurate and complete model for the atmosphere which includes the effect of ozone on the sky color, and an accurate description of the distribution of molecules. Our work follows a similar, explicit brute-force approach, and builds on similar sky representations. However, in contrast to previous work we focus on accurately describing not only an average stationary model of the atmosphere, but also the temporal and geographic dependence of the composition of the atmosphere.

Analytical models As opposed to explicitly modeling the distribution of particles in the atmosphere, analytical models express the radiance distribution on the sky-dome as a function. These models assume that the appearance of the sky is parametrized only by the view direction, as an environment map, and have been very successful for architectural purposes [CIE04, PSM93]. Preetham et al. [PSS99] introduced a colored parametric model suitable for graphics, parametrized by the turbidity of the atmosphere (i.e. the ratio between molecules and aerosols). Wilkie et al. [WUT*04] built over Preetham's model, introducing the polarization state of light in the model. Finally, Hosek and Wilkie [HW12] extended Preetham's model, making it more accurate under high turbidity conditions, introducing light reflected by the Earth's surface, extending the spectral sampling from RGB to hyperspectral rendering, and including an accurate depiction of the Sun in subsequent work [HW13]. All these works assume an idealized average atmosphere, with limited variability parametrized by the turbidity. In contrast, we account for the seasonal changes on the atmosphere, as well as the dependence on the location of the observer.

Other atmospheric phenomena Beyond the light transport in the clear atmosphere, significant work has been devoted to render clouds efficiently [BNM*08, ERWS12, ERDS14, KMM*17]. Although clouds can be considered as a dense concentration of the atmosphere's aerosols, their high frequency features lead to model them independently from the atmosphere, being illuminated by a given sky model. Sadeghi et al. [SML*12] developed a physically-based model for rainbows, by devising specific scattering functions for water droplets beyond Lorentz-Mie theory. Finally, Ishikawa et al. [IYI*11] proposed a data-driven empirical model for rendering aurora borealis.

3. Background

Light transport in the atmosphere is governed by the radiative transfer equation [Cha60], which in its differential form models the change in spectral radiance L for a given wavelength λ at point $\mathbf{x}$ in direction $\overrightarrow{\omega_o}$ as

$$(\overrightarrow{\omega_o}\cdot\nabla)L(\mathbf{x},\overrightarrow{\omega_o},\lambda) = -\mu_t(\mathbf{x},\lambda)L(\mathbf{x},\overrightarrow{\omega_o},\lambda) + \mu_s(\mathbf{x},\lambda)\int_{S^2} f(\mathbf{x},\overrightarrow{\omega_i}\rightarrow\overrightarrow{\omega_o},,\lambda)L(\mathbf{x},\overrightarrow{\omega_i},\lambda)\mathrm{d}\overrightarrow{\omega_i}, \quad (1)$$

where $\mu_t(\mathbf{x},\lambda) = \mu_a(\mathbf{x},\lambda) + \mu_s(\mathbf{x},\lambda)$ is the extinction coefficient at $\mathbf{x}$ for wavelength λ, and $\mu_a(\mathbf{x},\lambda)$ and $\mu_s(\mathbf{x},\lambda)$ are the absorption and scattering coefficients, respectively. The phase function $f(\mathbf{x},\overrightarrow{\omega_i}\rightarrow\overrightarrow{\omega_o},\lambda)$ is a probability distribution defined in the unit sphere S^2 modeling how light incoming from direction $\overrightarrow{\omega_i}$ is scattered towards direction $\overrightarrow{\omega_o}$ at $\mathbf{x}$. The boundary conditions defining the differential equation are the source term (i.e. the incoming light from the Sun and other sources) at the boundary of the medium, and the light reflected at the Earth surface, modeled by the rendering equation [Kaj86].

The extinction coefficient (and consequently the absorption and scattering coefficients) is defined in m^{-1} as $\mu_t(\mathbf{x},\lambda) = C_t(\mathbf{x})\,\sigma_t(\mathbf{x},\lambda)$, where the concentration $C_t(\mathbf{x})$ is the particles number per volume in m^{-3}, and $\sigma_t(\mathbf{x},\lambda)$ is the averages particles cross section in m^2. Note that we are assuming that the scattering is inelastic, and therefore there are no energy transfer between wavelengths as a consequence of e.g. fluorescence. An additional assumption in Equation (1) is that particles within the medium are uncorrelated. This means that for media made of a mixture of particles (as Earth's atmosphere), the extinction concentration $C_t(\mathbf{x})$ and

cross section $\sigma_t(\mathbf{x},\lambda)$ are

$$C_t(\mathbf{x}) = \sum_{j \in M} C_t^j(\mathbf{x}), \tag{2}$$

$$\sigma_t(\mathbf{x},\lambda) = \sum_{j \in M} \frac{C_t^j(\mathbf{x})}{C_t(\mathbf{x})} \sigma_t^j(\mathbf{x},\lambda), \tag{3}$$

where $C_t^j(\mathbf{x})$ and $\sigma_t^j(\mathbf{x},\lambda)$ are the concentration and cross section for particle j in the mixture M. This is analogous for scattering and absorption. Finally, we can define the phase function of the aggregate $f(\mathbf{x},\overrightarrow{\omega_i} \rightarrow \overrightarrow{\omega_o},\lambda)$ as

$$f(\mathbf{x},\overrightarrow{\omega_i} \rightarrow \overrightarrow{\omega_o},\lambda) = \sum_{j \in M} \frac{\mu_s^j(\mathbf{x},\lambda)}{\mu_s(\mathbf{x},\lambda)} f^j(\mathbf{x},\overrightarrow{\omega_i} \rightarrow \overrightarrow{\omega_o},\lambda), \tag{4}$$

with $\mu_s^j(\mathbf{x},\lambda)$ and $f^j(\mathbf{x},\overrightarrow{\omega_i} \rightarrow \overrightarrow{\omega_o},\lambda)$ the scattering coefficient and phase function of particle j. In summary, in order to render our atmospheric model, we need to define the concentration and optical parameters (scattering and absorption cross section, phase function) of the particles forming the atmosphere.

4. Our model

Here we define the optical properties of the atmosphere, so that we can move from a physical definition of the atmosphere to the optical parameters usable in the RTE [Equation (1)]. Similar to previous work, we assume that the atmosphere is composed by two main types of particles: molecules and aerosols. The former are the gases present in the atmosphere, mainly Nitrogen and Oxygen, and have very small size (significantly smaller than the light wavelength λ). They are responsible of the color of the atmosphere, and present a very homogeneous spatial distribution. Molecules are in general perfect scatterers, with the exception of ozone, which absorbs all incoming light. The aerosols, on the other hand, are larger suspended particles from different sources (dust, condensed water, human-made pollution...), located in the lower parts of the atmosphere, and that vary significantly depending on the position in the planet.

Therefore, we assume that the atmosphere is made of three particles: molecular scatterers, ozone, and aerosols. This allows us to formulate the optical properties of the media as [Equations (2) to (4)]

$$\mu_a(\mathbf{x},\lambda) = \mu_a^o(\mathbf{x},\lambda) + \mu_a^a(\mathbf{x},\lambda), \tag{5}$$

$$\mu_s(\mathbf{x},\lambda) = \mu_s^m(\mathbf{x},\lambda) + \mu_s^a(\mathbf{x},\lambda), \tag{6}$$

$$f(\mathbf{x},\overrightarrow{\omega_i} \rightarrow \overrightarrow{\omega_o},\lambda) = \frac{\mu_s^m(\mathbf{x},\lambda)}{\mu_s(\mathbf{x},\lambda)} f^m(\mathbf{x},\overrightarrow{\omega_i} \rightarrow \overrightarrow{\omega_o},\lambda) + \frac{\mu_s^a(\mathbf{x},\lambda)}{\mu_s(\mathbf{x},\lambda)} f^a(\mathbf{x},\overrightarrow{\omega_i} \rightarrow \overrightarrow{\omega_o},\lambda), \tag{7}$$

where the superscripts o, m and a stand for ozone, scattering molecules, and aerosols, respectively. In the following we detail the structure of the atmosphere, and how each of these terms are computed.

4.1. Structure

We model the atmosphere as a set of concentric spherical layers around the Earth, which we assume perfectly spherical, with radius 6360 km. We assume the Earth to have a diffuse reflectance, with varying albedo dependent on the type of surface around the observer. As shown by Hosek and Wilkie [HW12], the surface's albedo has a major impact on the appearance of the sky.Each layer in the atmosphere has different composition and thickness, with density varying as a function of pressure and temperature [Buc95]. The innermost layer, and closest to the Earth's surface, is the *troposphere*, where most molecules and aerosols concentrate, and with thickness of around 10 km. Above it we can find the *stratosphere*, composed mainly of molecules with the notable exception of certain aerosols in high mountain areas [AIA99]. This layer lasts up to 50 km over the sea level. Finally, over the stratosphere we can find the mesosphere, which extends up to around 80 km over the sea, and that has a very low density of scattering molecules and almost no aerosols. Notably, in the last kilometers of the mesosphere we can find the ozone layer. While after the *mesosphere* there exist some thin atmospheric layers (exosphere, termosphere), for computational purposes we define the end of the atmosphere at the Kármán line [San04], an imaginary line at 100 km over the sea level.

We chose the concentric spheres model over other simpler ones, such as the plane-parallel model typically used in atmospheric sciences [Cha60], because it does not introduce much complexity to our simulations, and allow us to realistically render dusk conditions, where the Earth cast a visible shadow on the atmosphere.

4.2. Molecular scattering

Molecular scattering is the main responsible of the color of the sky, including the reddish tone during twilight. It is the result of the scattering of light with molecules in the atmosphere, mainly Nitrogen and Oxygen, and is modeled by *Rayleigh* scattering [Str71]. This type of scattering is highly dependent on the wavelength, and has a diffuse behavior on the angular domain. The distribution of molecules is particularly steady, and does not vary significantly with respect of the position along the globe (see [Buc95] for the differences on Rayleigh optical depth as a function of latitude and season). However, it is strongly dependent on its vertical position on the atmosphere, since the concentration of molecules is dependent on the temperature and pressure at $\mathbf{x}$. This allows us to simplify the dependence on $\mathbf{x}$ to just its vertical component z. Scattering molecules do not absorb light significantly, which allows us to assume $\mu_a(\mathbf{x},\lambda)^m = 0$ for λ in the range between near infrared and ultraviolet light. Therefore, our goal is to model $\mu_s^m(z,\lambda)$ and $f^m(z,\overrightarrow{\omega_i} \rightarrow \overrightarrow{\omega_o},\lambda)$.

We compute the former by using the relationship $\mu_s^m(z,\lambda) = C_s^m(z)\,\sigma_s^m(\lambda)$, where $C_s^m(z)$ is the concentration of molecules as a function of height z, and $\sigma_s^m(\lambda)$ is the molecules' cross section, which is strongly dependent on λ. We compute the $C_s^m(z)$ using the 1976 U.S. Standard Atmosphere [Atm76], which provides an average model of the density of the atmosphere with respect to z. For the cross section $\sigma_s^m(\lambda)$, we follow the formulation proposed by Bucholtz [Buc95], and model it as

$$\sigma_s^m(\lambda) = \frac{24\pi^3 \left(\eta_s(\lambda)^2 - 1\right)^2}{\left(\lambda^4 N_s^2 + 2\right)^2} F_k(\lambda), \tag{8}$$

where $\eta_s(\lambda)$ is the index of refraction for standard air [PR72], $N_s = 2.547\,43 \times 10^{25}\,\mathrm{m}^{-3}$ is the molecular number density, and $F_k(\lambda) = \frac{6+3\rho_n(\lambda)}{6-7\rho_n(\lambda)}$ is the King correction factor, with $\rho_n(\lambda)$ the depolarization factor accounting for the anisotropy of the air, which can be found in [Bat84].

For the phase function $f^m(z, \vec{\omega_i} \to \vec{\omega_o}, \lambda)$, we follow the observation that the classic Rayleigh phase function does fail on accounting the effect of depolarization anisotropy. Instead, we use the more precise form proposed by Chandrasekhar [Cha60],

$$f^m(\vec{\omega_i} \to \vec{\omega_o}, \lambda) = \frac{3}{16\pi\,(1+2\gamma(\lambda))}\left[1+3\gamma(\lambda)+(1-\gamma(\lambda))\cos^2\theta\right], \tag{9}$$

where $\cos\theta$ is the dot product between $\vec{\omega_i}$ and $\vec{\omega_o}$, and $\gamma(\lambda) = \frac{\rho_n(\lambda)}{2-\rho_n(\lambda)}$ accounts for the λ-dependent depolarization. Note that the phase function for Rayleigh scattering is independent on z.

4.3. Molecular absorption

Molecular absorption in the atmosphere is mainly due to ozone. It accumulates at the upper parts of the mesosphere, although it is present in the rest of the atmosphere in lower density. Ozone does not scatter light, and therefore we can set $\mu_s^o(\mathbf{x}, \lambda) = 0$. In order to define the absorption, we use again the relationship $\mu_a^o(z,\lambda) = C_a^o(z)\,\sigma_a^o(\lambda)$. As mention before, the concentration of ozone $C_a^o(z)$ peaks in the mesosphere. We used the data measured by Ramanathan and Kulkarni [RK53], although we introduce the temporal behavior observed by Dütch [Düt74] to account for the changes on the ozone distribution along seasons. This allows us to introduce the temporal domain t into the concentration as $C_a^o(z,t)$. The cross section $\sigma_a^o(\lambda)$ has a strong dependence on λ, with a higher absorption of high-energy radiation (blue light towards ultraviolet). For $\sigma_a^o(\lambda)$ we use the tabulated values measured by Gorshelev et al. [GSW*13]. Putting concentration and absorption together, we end up with a time-varying model of ozone absorption, with $\mu_a^o(z,t,\lambda) = C_a^o(z,t)\,\sigma_a^o(\lambda)$. Note that once again we assume independence on the longitude and latitude of the observer, and only account for the vertical domain z. Introducing the effect of spatial variability could be interesting, since it would allow modeling the effect of the Antartic ozone hole.

4.4. Aerosols extinction and scattering

Aerosols are suspended particles in the air, larger than the wavelength of light. They can be categorized by their origin: Natural aerosols are produced by natural processes, like dust or salty water carried by the wind, or condensed gases like water drops in clouds, sulfates, or acids, while man-made aerosols like soot or pollution are made by human processes. The optical properties of aerosols, as well as their distribution, are very dependent on their nature and the location. For example, aerosols in the sea are very different from those in a large city. This complexity means that we cannot use a single optical parameter, but we need to create a mixture of different aerosols, in a similar fashion as Equations (2) to (4). In the following, we describe the generic framework we use for computing the optical parameters of a single aerosol; then, we generalize them to the different ambient conditions imposed by the position of the observer.

Optical properties of aerosols While aerosols are very different depending on their origin, we made the simplifying assumption of solid, spherical aerosols, with optical properties defined by their (complex) index of refraction η. This allows us to compute the optical properties of an aerosol particle p (σ_a^p, σ_s^p, and f^p) using Lorentz-Mie theory [Hul57]. Lorentz-Mie theory bases on an analytical solution of Maxwell Equations for spherical dielectric particles as an infinite sum of Legendre polynomials. It is able to accurately compute the scattering field, and scattering and absorption cross sections of a single particle, including high-frequency electromagnetic effects such as interference. This results into a very complex and detailed phase function (we refer to other sources e.g. [FCJ07] for details). While simpler phase functions (e.g. the Henyey-Greenstein phase function [HG41] or von Mishes-Fisher mixtures [GXZ*13]) have been proposed to reduce its complexity, we opt for sticking to the most accurate phase function possible, to faithfully represent the effect of the geographic location on aerosols.

Types of aerosol As mentioned before, the distribution and composition of aerosols in the atmosphere is very dependent on ambient factors, and therefore on the area in which they are measured. This imposes a heavy geographic dependence on our model. Based on Zimmermann et al. [ZFR*89] we account for six different types of areas with respect to their aerosol composition: POLAR, BACKGROUND, MARITIME, CONTINENTAL, DESERT, RURAL, and URBAN. Each of these types is a mixture of different aerosol components, which we categorize in ten major sets, following Jaenicke [Jae93]: Dust-like, Water-soluble, Soot, Sea-salt, Mineral, Sulfuric Acid, Volcanic ash, Meteoric, Sulfate, and Biogenic. The composition of aerosols vary with respect to the layer of the atmosphere. See Table 1 for the particular mixture of aerosol components for each type of area.

Distribution of aerosols In order to compute the optical properties of each type of aerosol based on Lorentz-Mie theory we need to specify both the radii of each particle, and their index of refraction. Defining a phase function for a single aerosol particle c as $f(\eta_c, r_c)$, with η_c the particle's complex index of refraction, and r_c its size, we can compute the average phase function f (we remove the spatial, directional and spectral dependence for clarity) as

$$f = \sum_{c\in T} w_c \int_0^\infty f(\eta_c, r) D_c(r)\mathrm{d}r, \tag{10}$$

where w_c is the proportion of a component c into an aerosol type T (see Table 1), with $\sum_{c\in T} w_c = 1$, and $D_c(r)$ is the distribution of sizes for a component c. By assuming that all aerosol components have roughly the same size distribution, we end up computing f as

$$f = \int_0^\infty D(r) \sum_{c\in T} w_c f(\eta_c, r)\mathrm{d}r. \tag{11}$$

We model $D(r)$ as a sum of three log-normal distributions, with the parameters specified in [AIA99, Table 10]. Finally, we use the measured complex indices of refraction $\eta_c(\lambda)$ for each component

given by D'Almeida et al. [DSK91]. The scattering and absorption cross sections σ_a and σ_s are computed analogously.

Vertical distribution of aerosols Finally, we need to define the concentration of aerosols, which is not constant along the vertical axis z, but fastly vanishes to zero as z increases. Following Jaenicke [Jae93], we model the vertical distribution of aerosols as $C_t^a(z)$:

$$C_t^a(z) = C_t^a(0)\left(\exp\left(\frac{-z}{H_p}\right) + \left(\frac{C_b}{C_t^a(0)}\right)^v\right)^v, \qquad (12)$$

where $C_t^a(0)$ is the aerosols concentration at the ground, C_b a background concentration value, H_p a height scaling parameter, and $v = \text{sign}(H_p)$. This formulation is very similar to the typical exponential distribution used in previous work, but introduces additional degrees of freedom for matching arbitrary types of aerosol distributions. Both C_b and H_p are specific for each type of aerosol, and therefore depend on the geographic location in which the observed is placed. In our work, we have used the parameters specified in [AIA99, Table 14].

5. Results

Here we demonstrate our model by rendering a set of hemispheric views of the sky dome rendered using a fisheye camera. All renderings have been done using path tracing, with Woodcock tracking for sampling vertices in the path, and next-even estimation for connecting path's vertices with the Sun using ratio tracking [NSJ14] for estimating the transmittance. For efficiency, we precompute both the phase functions and the z-resolved densities, and tabulate them for run-time query. We used brute-force spectral rendering with 81 samples in the range from 380 to 780 nm (a sample each 5 nm). All renders have been done in an Intel Core i5-6200U, with 8GB of RAM. The render time ranges between 30 minutes and 3 hours, with varying sample-rate depending on the variance of the image (e.g. twilight conditions were in general more noisy than daylight renders). Unless stated otherwise, we used an average surface albedo of 0.6, and set the month to June.

We compare the effect of the spatial dependence on the appearance of sky in Figures 1 and 2: Figure 1 compare the appearance in different locations, which results in different types of aerosols, at different sun elevations. In Figure 2 where we compare the atmospheric conditions in DESERT and URBAN environments, at low and high turbidities, respectively. As the turbidity increases, and therefore the amount of aerosols in the atmosphere, the effect introduced by the different aerosols gets more evident.

Figure 3 shows renders of the sky in a REMOTE CONTINENTAL area, with relatively low turbidity, for different twilight conditions (i.e. with the Sun under the horizon). Our model can realistically predict the appearance of the sky, even in challenging conditions such as dusk. Figure 4 shows a similar scene, with a cylindrical mapping of the sky-dome. In these renders we can see clearly the projected shadow of the Earth on the atmosphere during twilight, and how it progressively diffuses due to scattering.

The temporal dependence of our model with respect of the time of the year is demonstrated in Figure 5, where we compare the appearance of the atmosphere at dusk in a CLEAN MARITIME environment with low turbidity, for the months of January (higher density of ozone) and November (lower density of ozone). The amount of ozone is responsible of higher absorption at higher frequencies, which results in a more vivid color of the atmosphere when higher concentration of ozone is present.

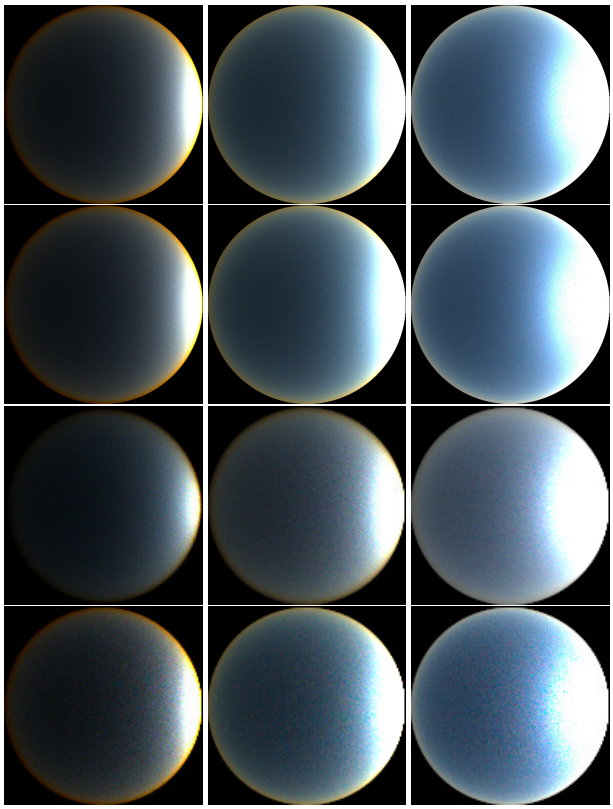

Figure 2: Renders for different types of aerosols, at different turbidities, and with different sun elevation (from left to right, 0°, 5° and 25°). From top to bottom: DESERT and URBAN with low turbidity, and DESERT and URBAN with high turbidity. As the density of aerosols increases, the differences between the two types of aerosols and their effect on the appearance of the sky increase.

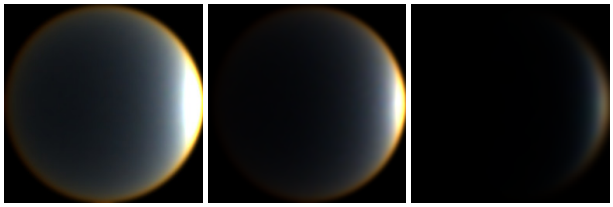

Figure 3: Renders of the sky on a REMOTE CONTINENTAL area, with sun elevations of, from left to right, $-0.5°$, $-2.5°$ and $-5°$ with respect to the horizon.

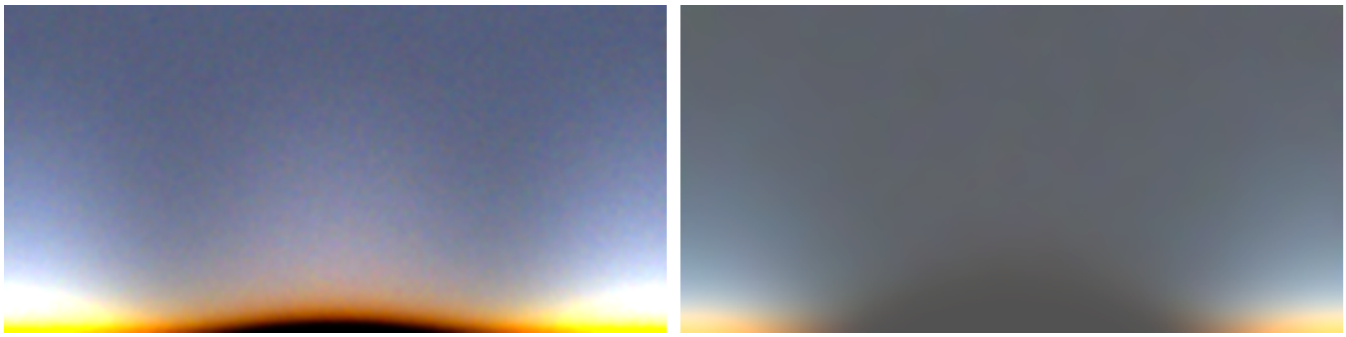

Figure 4: Renders of the sky in a REMOTE CONTINENTAL region, using a hemispherical camera with cylindrical mapping of the sky-dome (the zenith is at the top of the image). The sun has elevation of -2.5° (left) and -5° (right) with respect to the horizon. Here we can clearly see the Earth's shadow projected on the atmosphere, which is specially visible at twilight conditions.

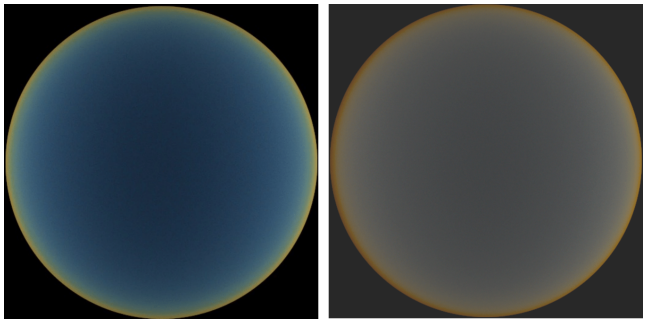

Figure 5: Differences on the appearance of the atmosphere due to temporal variability of ozone concentration at a CLEAN MARITIME location, and very low aerosol concentration, for measurements at January (left) and November (right). The sun elevation is -5°.

Figure 6 shows the spectral renders of the atmosphere as a function of light wavelength, for different sun elevations. We can see how shorter wavelengths have in general higher intensity in daytime, and as the sun approximates to the horizon the intensity is significantly reduced in the zenith, with the horizon being significantly brighter, specially in at the red part of the visible spectrum.

Finally, in Figure 7 we compare our model with the data captured by Kider et al. [KJKN*14], showing similar radiance gradients and color distribution. Note that there are several unknowns in Kider et al.'s data, including the atmosphere turbidity, actual type of aerosol (we assumed captures were performed at a URBAN area), time of the year, and camera and tone-mapping parameters; while these uncertainties, together with some implicit simplifications of our model, might introduce some differences on the images, our results look plausibly similar to the data captured by Kider and colleagues.

6. Conclusions

In this work we have presented an atmospheric model that takes into account changes on appearance in the sky due to temporal (seasonal) and spatial variations in the atmosphere. For that, we have built a detailed model of the atmosphere, including scattering molecules, ozone, and aerosols, and precisely modeling their distribution and optical behavior. We base our model in an extensive review of the atmospheric science literature, using accurate measurements and optical models to move from the atmospheric composition to optical properties, that can be rendered in any volumetric render engine. Our work gives a new step towards the final goal of fully accurate skies in computer graphics.

Limitations and Future Work Despite the accuracy in terms of the description of the optics of the atmosphere, our work presents some limitations. First of all, we are assuming that the rays traverse the atmosphere in straight lines. This is not true in the atmosphere, and in fact is the cause of several interesting phenomena, specially in twilight conditions. Given that our model already includes accurate temperature profiles of the atmosphere, it should be relatively easy to move from the standard RTE [Equation (1)] to its refractive counterpart [ABW14] with support for curved rays [GMAS05]. Another important limitation is the lack of support for polarization [JA18]. This is in fact significant, since scattering by molecules is highly polarizing, and in fact might introduce observable changes on the sky appearance [MLT94]. We are also assuming that the Sun is the only light source contributing to the atmosphere. While this assumption might be valid in daylight conditions, this is a rather severe limitation when rendering night skies. While introducing Jensen et al.'s [JDD*01] physically-based nigh light sources into our description of the atmosphere should be relatively straightforward, adding other types of light source, specially accurate and predictable human-made urban lighting, would require from precise measurements of light pollution. Adding support to high levels of turbidity (haze) is another interesting avenue of future work. At high concentration of aerosols, their distribution becomes affected by air turbulence. Therefore spatial correlation on aerosols particles appears. Accounting for such correlation would require departing from standard radiative transfer, and moving to generalized light transport [JAG18]. Finally, although the atmospheric composition in our model is based on measurements, and that the results look plausible, future work is needed to assess that our model accurately and predictively represents the atmosphere radiometrically. Although we have done some preliminary tests against the data measured by Kider et al. [KJKN*14] (Figure 7), more work is

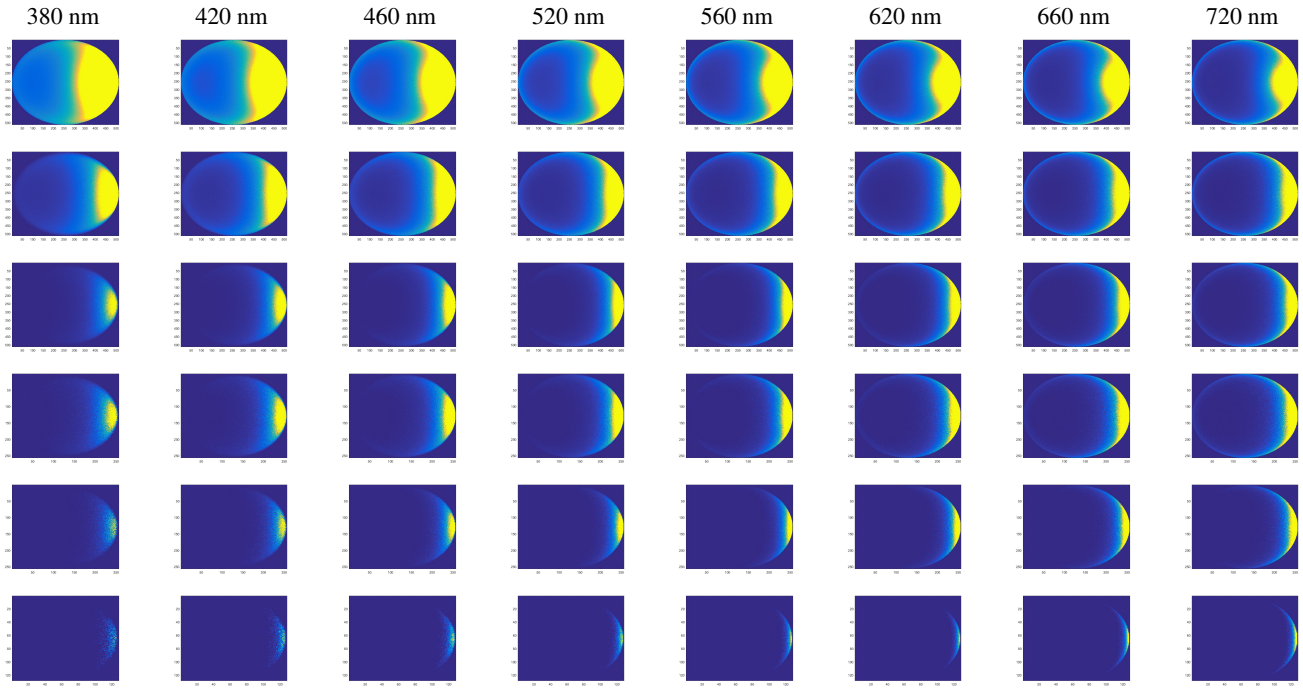

Figure 6: Spectral renderings of the sky-dome at different Sun elevations (from top to bottom: 25, 5, 0, -.5, -2.5, and -5°). Color codes spectral radiance. As the Sun goes down, the total radiance decreases, specially in the bluemost areas in the zenith.

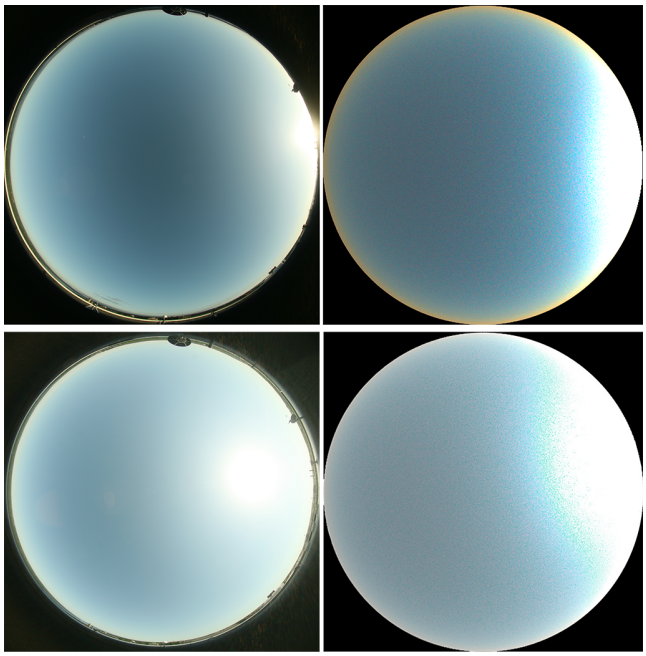

Figure 7: Comparison between the data captured by Kider et al. [KJKN*14] (left) and our rendered data for URBAN aerosols (right) for sun elevation of 5° (top) and 25° (bottom).

needed with precise calibration of the media. Following the procedure recently proposed by Bruneton [Bru17] is a promising direction for such evaluation.

Acknowledgements

We thank Philip Laven for providing the software *MiePlot*. This project has been funded by the European Research Council (ERC) under the EU's Horizon 2020 research and innovation programme (project CHAMELEON, grant No 682080), DARPA (project REVEAL), and the Spanish Ministerio de Economía y Competitividad (project TIN2016-78753-P).

References

[ABW14] AMENT M., BERGMANN C., WEISKOPF D.: Refractive radiative transfer equation. *ACM Trans. Graph. 33*, 2 (2014). 6

[AIA99] AIAA: *Guide to Global Aerosol Models*. American Institute of Aeronautics and Astronautics, 1801 Alexander Bell Drive, Reston, VA 22091, 1999. 3, 4, 5

[Atm76] ATMOSPHERE U. S.: Noaa, nasa, usaf. *Washington DC* (1976). 3

[Bat84] BATES D.: Rayleigh scattering by air. *Planetary and Space Science 32*, 6 (1984), 785–790. 4

[BN08] BRUNETON E., NEYRET F.: Precomputed atmospheric scattering. In *Computer Graphics Forum* (2008), vol. 27, Wiley Online Library, pp. 1079–1086. 2

[BNM*08] BOUTHORS A., NEYRET F., MAX N., BRUNETON E., CRASSIN C.: Interactive multiple anisotropic scattering in clouds. In *Proceedings of the 2008 symposium on Interactive 3D graphics and games* (2008), ACM, pp. 173–182. 2

Troposphere			
POLAR	Antartic	0.99	Sulfuric Acid
		0.005	Sea Salt
		0.005	Mineral
	Artic	0.25	Soot
		0.25	Sea Salt
		0.25	Mineral
		0.25	Sulfate
BACKGROUND		0.5	Sulfate
		0.5	Sulfuric Acid
MARITIME	Clean	0.6	Sea Salt
		0.4	Sulfate
	Polluted	0.6	Water Soluble
		0.4	Sea Salt
CONTINENTAL		0.3	Dust-Like
		0.3	Water Soluble
		0.3	Soot
DESERT		1.0	Mineral
RURAL		0.94	Water Soluble
		0.06	Soot
URBAN		0.6	Water Soluble
		0.4	Soot
Stratosphere			
BACKGROUND		1	Sulfuric Acid
VOLCANIC		0.5	Sulfuric Acid
		0.5	Volcanic Ash

Table 1: Contributing proportion on each aerosol types of each aerosol component [Jae93].

[Bru17] BRUNETON E.: A qualitative and quantitative evaluation of 8 clear sky models. *IEEE transactions on visualization and computer graphics 23*, 12 (2017), 2641–2655. 2, 7

[Buc95] BUCHOLTZ A.: Rayleigh-scattering calculations for the terrestrial atmosphere. *Applied Optics 34*, 15 (1995), 2765–2773. 3

[Cha60] CHANDRASEKHAR S.: Radiative transfer, ed. *Chandrasekhar, S 20* (1960). 1, 2, 3, 4

[CIE04] CIE S.: 011/e: 2003 spatial distribution of daylight-cie standard general sky, 2004. 2

[DSK91] D'ALMEIDA G. A., SHETTLE E. P., KOEPKE P.: *Atmospheric aerosols : global climatology and radiative characteristics*. A. Deepak Pub Hampton, Va., USA, 1991. 5

[Düt74] DÜTSCH H.: The ozone distribution in the atmosphere. *Canadian journal of chemistry 52*, 8 (1974), 1491–1504. 4

[EK10] ELEK O., KMOCH P.: Real-time spectral scattering in large-scale natural participating media. In *Proceedings of the 26th Spring Conference on Computer Graphics* (2010), ACM, pp. 77–84. 2

[ERDS14] ELEK O., RITSCHEL T., DACHSBACHER C., SEIDEL H.-P.: Principal-ordinates propagation for real-time rendering of participating media. *Computers & Graphics 45* (2014), 28–39. 2

[ERWS12] ELEK O., RITSCHEL T., WILKIE A., SEIDEL H.-P.: Interactive cloud rendering using temporally coherent photon mapping. *Computers & Graphics 36*, 8 (2012), 1109–1118. 2

[FCJ07] FRISVAD J. R., CHRISTENSEN N. J., JENSEN H. W.: Computing the scattering properties of participating media using lorenz-mie theory. *ACM Trans. Graph. 26*, 3 (2007). 4

[GMAS05] GUTIERREZ D., MUÑOZ A., ANSON O., SERON F.: Nonlinear volume photon mapping. In *Eurographics Symposium on Rendering '05* (2005). 6

[GSAM04] GUTIERREZ D., SERON F. J., ANSON O., MUÑOZ A.: Chasing the green flash: a global illumination solution for inhomogeneous media. In *Proceedings of the 20th spring conference on Computer graphics* (2004), ACM, pp. 97–105. 2

[GSW*13] GORSHELEV V., SERDYUCHENKO A., WEBER M., CHEHADE W., BURROWS J.: High spectral resolution ozone absorption cross-sections–part 1: Measurements, data analysis and comparison with previous measurements around 293k. *Atmospheric Measurement Techniques Discussions 6*, 4 (2013). 4

[GXZ*13] GKIOULEKAS I., XIAO B., ZHAO S., ADELSON E. H., ZICKLER T., BALA K.: Understanding the role of phase function in translucent appearance. *ACM Transactions on Graphics (TOG) 32*, 5 (2013), 147. 4

[HG41] HENYEY L. G., GREENSTEIN J. L.: Diffuse radiation in the Galaxy. *Astrophysical Journal 93* (Jan. 1941), 70–83. doi:10.1086/144246. 4

[HMS05] HABER J., MAGNOR M., SEIDEL H.-P.: Physically-based simulation of twilight phenomena. *ACM Transactions on Graphics (TOG) 24*, 4 (2005), 1353–1373. 1, 2

[Hul57] HULST H. C.: *Light scattering by small particles*. Courier Corporation, 1957. 4

[HW12] HOSEK L., WILKIE A.: An analytic model for full spectral sky-dome radiance. *ACM Transactions on Graphics (TOG) 31*, 4 (2012), 95. 1, 2, 3

[HW13] HOSEK L., WILKIE A.: Adding a solar-radiance function to the hosek-wilkie skylight model. *Computer Graphics and Applications, IEEE 33*, 3 (2013), 44–52. 2

[IYI*11] ISHIKAWA T., YUE Y., IWASAKI K., DOBASHI Y., NISHITA T.: Modeling of aurora borealis using the observed data. In *Proceedings of the 27th Spring Conference on Computer Graphics* (2011), ACM, pp. 13–16. 2

[JA18] JARABO A., ARELLANO V.: Bidirectional rendering of vector light transport. *Computer Graphics Forum* (2018). 6

[Jae93] JAENICKE R.: *Tropospheric Aerosols in Aerosol-Cloud-Climate Interactions,*. P.V. Hobbs, Academic Press, 1993. 4, 5, 8

[JAG18] JARABO A., ALIAGA C., GUTIERREZ D.: A radiative transfer framework for spatially-correlated materials. *ACM Trans. Graph. 37*, 4 (2018). 6

[JDD*01] JENSEN H. W., DURAND F., DORSEY J., STARK M. M., SHIRLEY P., PREMOŽE S.: A physically-based night sky model. In *Proceedings of the 28th annual conference on Computer graphics and interactive techniques* (2001), ACM, pp. 399–408. 1, 2, 6

[Kaj86] KAJIYA J. T.: The rendering equation. In *ACM Siggraph Computer Graphics* (1986), vol. 20, ACM, pp. 143–150. 2

[KJKN*14] KIDER JR J. T., KNOWLTON D., NEWLIN J., LI Y. K., GREENBERG D. P.: A framework for the experimental comparison of solar and skydome illumination. *ACM Transactions on Graphics (TOG) 33*, 6 (2014), 180. 2, 6, 7

[KMM*17] KALLWEIT S., MÜLLER T., MCWILLIAMS B., GROSS M., NOVÁK J.: Deep scattering: rendering atmospheric clouds with radiance-predicting neural networks. *ACM Transactions on Graphics (TOG) 36*, 6 (2017), 231. 2

[Kut12] KUTZ P. Z.: Physically-based atmosphere rendering. 2

[MLT94] MISHCHENKO M., LACIS A., TRAVIS L.: Errors induced by the neglect of polarization in radiance calculations for rayleigh-scattering atmospheres. *Journal of Quantitative Spectroscopy and Radiative Transfer 51*, 3 (1994), 491–510. 6

[NDKY96] NISHITA T., DOBASHI Y., KANEDA K., YAMASHITA H.: Display method of the sky color taking into account multiple scattering. In *Pacific Graphics* (1996), vol. 96, pp. 117–132. 1, 2

[NGHJ18] NOVÁK J., GEORGIEV I., HANIKA J., JAROSZ W.: Monte carlo methods for volumetric light transport simulation. *Computer Graphics Forum (Proceedings of Eurographics - State of the Art Reports) 37*, 2 (May 2018). 1, 2

[NSJ14] NOVÁK J., SELLE A., JAROSZ W.: Residual ratio tracking for estimating attenuation in participating media. *ACM Transactions on Graphics (TOG) 33*, 6 (2014), 179. 5

[NSTN93] NISHITA T., SIRAI T., TADAMURA K., NAKAMAE E.: Display of the earth taking into account atmospheric scattering. In *Proceedings of the 20th annual conference on Computer graphics and interactive techniques* (1993), ACM, pp. 175–182. 2

[O'N05] O'NEIL S.: Accurate atmospheric scattering. *GPU Gems 2* (2005), 253–268. 2

[PR72] PECK E. R., REEDER K.: Dispersion of air*. *JOSA 62*, 8 (1972), 958–962. 4

[PSM93] PEREZ R., SEALS R., MICHALSKY J.: All-weather model for sky luminance distribution–preliminary configuration and validation. *Solar energy 50*, 3 (1993), 235–245. 2

[PSS99] PREETHAM A. J., SHIRLEY P., SMITS B.: A practical analytic model for daylight. In *Proceedings of the 26th annual conference on Computer graphics and interactive techniques* (1999), ACM Press/Addison-Wesley Publishing Co., pp. 91–100. 1, 2

[RK53] RAMANATHAN K., KULKARNI R.: Height distribution of atmospheric ozone. In *Proceedings of the Indian Academy of Sciences-Section A* (1953), vol. 37, Springer, pp. 321–331. 4

[San04] SANZ FERNÁNDEZ S.: 100km altitude boundary for astronautics, June 2004. Published in Fédération Aéronautique Internationale. URL: http://www.fai.org/icare-records/100km-altitude-boundary-for-astronautics. 3

[SML*12] SADEGHI I., MUNOZ A., LAVEN P., JAROSZ W., SERON F., GUTIERREZ D., JENSEN H. W.: Physically-based simulation of rainbows. *ACM Transactions on Graphics (Presented at SIGGRAPH) 31*, 1 (Feb. 2012), 3:1–3:12. doi:10.1145/2077341.2077344. 2

[Str71] STRUTT J. W.: On the scattering of light by small particles. *The London, Edinburgh, and Dublin Philosophical Magazine and Journal of Science 41*, 275 (1871). 3

[TS99] THOMAS G. E., STAMNES K.: *Radiative transfer in the atmosphere and ocean*. Cambridge atmospheric and space science series. Cambridge University Press, Cambridge, New York, 1999. Autre tirage : 2002. URL: http://opac.inria.fr/record=b1095234. 2

[WUT*04] WILKIE A., ULBRICHT C., TOBLER R. F., ZOTTI G., PURGATHOFER W.: An analytical model for skylight polarisation. In *Rendering Techniques* (2004), pp. 387–398. 2

[ZFR*89] ZIMMERMANN P., FEICHTER J., RATH H., CRUTZEN P., WEISS W.: A global three-dimensional source-receptor model investigation using 85kr. *Atmospheric Environment 23*, 1 (1989), 25–35. 4